Energy Economics 126 (2023) 106923

Contents lists available at ScienceDirect

Energy Economics

journal homepage: www.elsevier.com/locate/eneeco

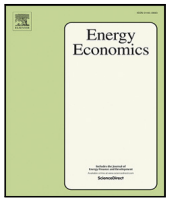

Intensive and extensive margins of the peak load: Measuring adaptation with mixed frequency panel data

Francesco Pietro Colelli [a,b,*], Ian Sue Wing [c], Enrica De Cian [a,b]

[a] Department of Economics, Ca' Foscari University of Venice, 30121 Venice, Italy
[b] Centro Euro-Mediterraneo sui Cambiamenti Climatici (CMCC), 30175 Venice, Italy
[c] Boston University, MA 02215, United States

ARTICLE INFO

JEL classification:
C1
Q00
Q40
Q41
Q47
Q54

Keywords:
Energy
Adaptation
Climate change
Air-conditioning

ABSTRACT

In this work we investigate the response of daily electricity peak load to daily maximum temperatures across states in Europe and India. We propose a method that decomposes short- from medium/long-run effects, retains the high frequency nature of the load-weather covariation and treats economic growth as a modulating factor. By simultaneously exploiting variation in unexpected daily weather anomalies and decade-long climatic changes in each location we decompose transitory - intensive margin - adjustments from permanent - extensive margin - adjustments. We find that the shocks over the long-run differ substantially from the short-run dynamics. Furthermore, we find evidence that per capita income modulates the adjustments over the short- and long-run. We project that in response to climate change around 2050 the peak load may increase by up to 20%-30% in Southern Europe and in several states in India, depending on the degree of warming and the evolution of socio-economic conditions. Even with a limited scope to two world regions, we identify that the structure of the economy and differences in future income growth matter in shaping the adaptation to climate change. Our decomposition allows to identify how future weather anomalies can further amplify the relative increase associated to the shift in the climate norm. Assuming that the interannual variability of maximum temperatures follows the distribution observed in the past, we find a doubling of the impacts of climate change during the summer in Europe. Uncertainty around the distribution of future weather anomalies may lead to further unexpected peak load amplifications. Our results have important policy implications for power systems' generation capacity, transmission and storage, as we show that the challenges to accommodate the peak load in days with extreme temperatures may substantially increase already around mid-century.

1. Introduction

Electric power systems' generation capacity, transmission, and storage are designed to meet peak load, the maximum quantity of electricity instantaneously demanded by grid-connected customers. Electricity consumption is highly weather-sensitive (Yalew et al., 2020), with demands for heating and cooling determining seasonal peak loads (Boßmann and Staffell, 2015). Air-conditioning (AC) accounts for 30% of peak demand in temperate and industrialized countries such as the United States, and for 10% to 15% in tropical regions such as India, Indonesia, and Mexico (International Energy Agency, 2018). Particularly in emerging economies, AC adoption is expected to rise rapidly due to the higher temperatures and growing per-capita income (Davis et al., 2021; Pavanello et al., 2021). In this context, a major concern is that the more frequent and intense extreme temperature events that are projected in the near future (Seneviratne et al., 2021) will push energy demand to levels that exceed system capacity more often, adversely affecting electricity grids' ability and reliability to deliver power, with non-negligible implications for mortality and morbidity (Stone et al., 2023). Key questions are thus the magnitude, character, and timing of investments in electricity generation, transmission, and distribution capacity that will be needed to accommodate the combination of these short- and long-run adjustments, and what the implications might be for future power system reliability and greenhouse gas (GHG) emissions (Barnett and O'Neill, 2010). Load forecasting is fundamental to addressing these questions. In the short run, actual load exceeding forecasted demand incurs costs in the form of balancing services, load shedding, or, at worst, unplanned outages. Long-run peak load forecasts are critical for planning generation, transmission, and distribution capacity additions and retirements on multi-year horizons. While operational forecasts only take into account historically-observed weather patterns (Moral-Carcedo and Pérez-García, 2017; Lindberg et al., 2019), empirical projections of future electricity demand generally lack the spatial

* Corresponding author at: Department of Economics, Ca' Foscari University of Venice, 30121 Venice, Italy.
E-mail address: francesco.colelli@unive.it (F.P. Colelli).

https://doi.org/10.1016/j.eneco.2023.106923
Received 23 January 2023; Received in revised form 17 July 2023; Accepted 26 July 2023
Available online 4 August 2023

and temporal precision to inform power system planning (Deschênes and Greenstone, 2011; Aroonruengsawat and Auffhammer, 2011; De Cian and Sue Wing, 2019), or are limited in their ability to capture the potential moderating effects of climate change adaptation (Wenz et al., 2017; Auffhammer et al., 2017; Rode et al., 2021; Auffhammer, 2022a).

Empirical models that infer climate impacts from co-variation between economic outcomes and weather fluctuations may not accurately capture the true long-run effects of climate change (Dell et al., 2014). People respond to temperature shocks by adjusting their utilization of energy-consuming capital goods such as AC. Changes in the utilization of a capital good that is fixed in the short run are referred to as the 'intensive margin'. Over longer time frames, repeated temperature regimes that agents perceive to be climatic shifts can induce adjustments in the possessions of durable stocks, e.g., households without AC purchasing an air conditioner. Such adjustments are referred to as the 'extensive margin' (Auffhammer and Mansur, 2014). Adjustments along the extensive margin show their impacts over a longer period of time and because capital goods are fixed character in the short run, actors' responses to unanticipated weather shocks mostly through the intensive margin.

Fine temporal scale co-variation between load and temperature identifies the intensive-margin effects of transient extreme heat exposures, conditional on electricity consumers' adjustments to their utilization of durable stocks that are quasi-fixed (Wenz et al., 2017; Auffhammer et al., 2017; Fonseca et al., 2019; Romitti and Sue Wing, 2020). The central challenge is to identify simultaneous adjustments along the extensive margin, i.e., consumer responses to average weather conditions experienced over many years, in the form of new technology adoption and/or adjustment of stocks of appliances with varying energy efficiencies—which are seldom directly observed (compare Davis and Gertler, 2015; Auffhammer, 2022b). The framework proposed by Auffhammer (2022a) quantifies extensive margin adjustments with no information on the stock of appliances, but exploits cross-sectional variation across several thousand households and henceforth relies on rarely available large billing datasets.

In this paper, we propose a methodology to disentangle the intensive- and extensive-margin adaptation components that are latent in the relationship between electricity demand and temperature.

Departing from the common approach that treats economic, technological, and demographic trends as unobserved confounders (Auffhammer et al., 2017; Wenz et al., 2017), our strategy distinguishes the responses of peak load to high-frequency transitory departures of daily maximum temperatures from their climatic normal values (which capture the effects of changes in appliance utilization) from those to the low-frequency, interannual evolution of decadal average daily maximum temperatures and per-capita income (which capture the effects of growth, and/or improvements in the efficiency of, appliance stocks). Our motivating hypothesis is that income affects consumers' responses to climatic and weather shocks by determining their low-frequency adjustment of energy-using capital goods like appliances and air conditioners, and the high-frequency intensity of utilization of those durables. We couple the resulting short- and long-run electric load responses to temperature with projections of mid-century changes in daily maximum temperatures simulated by 25 global climate models (GCMs) to elucidate the potential future intensive- and extensive-margin effects on electricity consumption in Europe and India.

2. Modeling climate adaptation: Conceptual and empirical frameworks

The total load on the power grid results from the electricity demand that is unrelated to ambient weather or climate conditions (e.g., cooking, manufacturing processes) and from electricity usages that are sensitive to meteorological conditions (e.g., operation of electrical heating, ventilation and cooling assets). Peak weather-sensitive electricity demand (q) can then be decomposed into a long-run extensive margin and a short-run intensive margin component (q_E and q_I, respectively):

$$q = f(q_E, q_I) \tag{1}$$

What varies along the extensive margin includes the size (a) and the technological characteristics ($\bar{\vartheta}$) of the space conditioning appliances, as well as their average level of utilization ($\bar{u}$). Per capita income (Y) and expected climate conditions (C) come into play by influencing all these three elements:

$$q_E = a(C,Y) \cdot \bar{\vartheta}(C,Y) \cdot \bar{u}(C,Y) = h(C,Y) \tag{2}$$

We assume that changes along the intensive margin only occur when the weather realization (T) diverges from the expected climate, $\mathbb{E}[T|C] \neq C$. We define the divergence of weather from the climatically-determined mean as an unanticipated weather anomaly ($\omega = \mathbb{E}[T|C] - C$). Such divergence induces adjustment along the intensive-margin via changes in the utilization of the fixed stock of assets. The short-run effect is constrained by the fixed durable stocks ($\bar{a}$) and their average use patterns ($\bar{\vartheta}$), while income facilitates the degree of actual utilization in response to anomalies ω:

$$q_I = \bar{a} \cdot \bar{\vartheta} \cdot u(\omega, Y) = g(C, Y, \omega; h(C,Y)) \tag{3}$$

Under the assumption of linear additivity, total electricity demand can be decomposed as follows:

$$q = h(C,Y) + g(C,Y,\omega; h(C,Y)) \tag{4}$$

which highlights the challenge of empirically disentangling the commingled effects of weather and climate.

Existing empirical modeling strategies address this challenge by following three broad categories of approaches (Dell et al., 2014; Kolstad and Moore, 2020). Cross-sectional approaches measure long-run adaptation by directly estimating a climate response function across locations characterized by different average climates. The specification is essentially a time-averaged approximation of Eq. (4) at different cross-sectional units (i):

$$\bar{q}_i \approx h(\bar{C}_i, \bar{Y}_i) + g(\bar{C}_i, \bar{Y}_i; h(\bar{C}_i, \bar{Y}_i)) \tag{5a}$$

$$\Rightarrow \bar{q}_i = f(\bar{C}_i) + \text{controls}_i + \varepsilon_i \tag{5b}$$

where overlined variables indicate averages over time. The underlying assumption is that welfare-maximizing agents will have fully adjusted their asset stocks, and utilization of them, to the mean climatic conditions they face (Mendelsohn et al., 1994; Schlenker et al., 2005). The well-understood drawback of this approach is its inability to control for time-invariant factors that are jointly correlated with the climate and the outcome variable, with the potential for omitted variable bias.

The second category is cross-section/time-series, or panel, models that exploit deviations of instantaneous weather from the location-specific average of weather over time, while the differences in climate, constant over time, are captured by location-specific fixed effects (Deschênes and Greenstone, 2011; Schlenker and Roberts, 2009), as shown in Eqs. (6a) and (6b). The advantage of this approach is the ability to control for idiosyncratic, time-invariant, locationally-varying shocks through the inclusion of cross sectional and time fixed effects (μ_i and σ_t, respectively). This approach has been widely used to investigate residential energy demand responses to temperature (Deschênes and Greenstone, 2011; Aroonruengsawat and Auffhammer, 2011; Auffhammer et al., 2017; Wenz et al., 2017). This approach is also vulnerable to the omission of time-varying factors that influence energy demand and are correlated over time with temperature (Hsiang et al., 2016). Moreover, the effects of low-frequency variations in the climate or climate-adaptive behavior over the cross-section is not identified due to collinearity with the fixed effects. The resulting responses identified out of inter-annual variations should be interpreted as the short-run intensive-margin adjustments that do not account for the consequences of more gradual extensive-margin adaptation. Non-linear specifications

of the weather variables, $f(T)$, allow the marginal effect of a given amount of warming to vary locationally (Schlenker and Roberts, 2009, 2006), but the identified effects are still a combination of long- and short-run responses (Kolstad and Moore, 2020):

$$q_{i,t} - \bar{q}_i \approx h(T_{i,t} - \overline{T}_i, Y_{i,t} - \overline{Y}_i) + g(T_{i,t} - \overline{T}_i, Y_{i,t} - \overline{Y}_i; h(T_{i,t} - \overline{T}_i, Y_{i,t} - \overline{Y}_i)) \tag{6a}$$

$$\Rightarrow q_{i,t} = f(T_{i,t}) + \mu_i + \sigma_t + \varepsilon_{i,t} \tag{6b}$$

A number of studies adopt hybrid approaches that aim to identify the impact of climate while still controlling for unobservable confounding variables, using a variety of methods (Kolstad and Moore, 2020). Two-stage, meta-analytic approaches (Butler and Huybers, 2013; Carleton et al., 2020; Auffhammer, 2022b) estimate, first, outcome variables' linear responses to weather over time for various locations, and, subsequently, the value of estimated weather coefficients as a function of climate using cross-sectional regressions. Distinctly, estimations based on long-differences (Burke and Emerick, 2016; Moore and Lobell, 2014), exploit the observations of medium-run change across locations over multiple periods and compare the effect on the outcome variable of such medium-term climatic changes to the effect of interannual variations. While differencing removes the effect of time-invariant biases, flexible time trends control for further omitted variables that affect both the trend in weather and outcome. Estimations following the inclusion of such controls gain statistical power from the effect of idiosyncratic variation in the long-term trends around the average (Kolstad and Moore, 2020).

Dynamic error correction modeling has sought to simultaneously identify temperature's effects on both long-run equilibrium energy demand and short-run adjustment towards that equilibrium (De Cian and Sue Wing, 2019).

Other approaches based on heterogeneous marginal effect frameworks identify adaptation by including a set of interaction terms that modulate the relation between the outcome and weather either though a cross-sectionally varying parameter. Examples include cross-sectional averages of climate as in Rode et al. (2021), Carleton et al. (2020), dummy variables grouping units by level of development as in Burke et al. (2015), or time-varying factors, such as income per capita levels as in Rode et al. (2021), Carleton et al. (2020). The modulation term of climate can be included only as a interaction parameter because of its perfect collinearity with the fixed effects μ_i. This specification can be generalized as an approximation to Eq. (4) that provides heterogeneous values of the intensive margin response over different average climatic cross-sectional exposure:

$$q_{i,t} = h(\overline{C}_i, \overline{Y}_i) + g(T_{i,t}, \overline{Y}_i; h(\overline{C}_i, \overline{Y}_i)) \tag{7a}$$

$$\Rightarrow q_{i,t} = f^T(T_{i,t}) + f^C(T_{i,t}) \cdot \overline{C}_i + f^Y(T_{i,t}) \cdot \overline{Y}_i + \mu_i + \sigma_t + \varepsilon_{i,t} \tag{7b}$$

The justification for the heterogeneous marginal effect approaches is that over the period of the sample there is not a sufficiently large within-unit variation in climate for the purposes of identification. Moving away from such assumption, Mérel and Gammans (Mérel and Gammans, 2021) and Bento et al. (Bento et al., 2020) use panel data and partition the variation in weather into a slowly-moving climate exposure ($\widetilde{C}$), where $\widetilde{C}$ identifies a form of time smoothing, such a multi-year moving average, and short-run weather deviations from it (ω), using the two distinct variables to jointly to estimate the effects of respectively long- and short-run effects:

$$\widetilde{C}_{i,t} = \frac{\sum_{n=t-k}^{t-1} T_{i,t}}{k} \tag{8}$$

$$\omega_{i,t} = T_{i,t} - \widetilde{C}_{i,t} \tag{9}$$

where: i indexes the unit, t indexes the time step, k indexes the moving average window.

The identification of any statistically significant adaptation adjustments is explicit since it is derived directly from the difference between the responses to weather shocks and climatic changes (Bento et al., 2021). Most importantly, since adaptation in the response is measured by the progressive adjustments of the same economic agents, this unifying approach does not require extrapolation over time and space to infer adaptation. The effect of weather shocks and climatic variations are identified by the variations over time in each location, that is the climate variable evolves not only across locations but also over time in each given location. The partitioning method proposed by Bento et al. (2020) can be straightforwardly applied to investigate differences in the intensive and extensive margins as theorized in Eq. (4) and to separate the effect of $\widetilde{C}$ and ω on q, identifying in the same equation the slowly evolving behavior resulting in the extensive margin effect and the instantaneous constrained adjustment resulting in the intensive margin effect.

Here we also aim at identifying the effect of socio-economic development. Considered as a non-temperature confounder, socio-economic development is typically removed through low frequency controls such as polynomials functions of time trends (Auffhammer et al., 2017; Wenz et al., 2017) or year dummies in a semi-parametric framework (Romitti and Sue Wing, 2020). Here we assume that we can identify the separate effects of a slowly moving socio-economic driver such as per capita income ($\widetilde{Y}$) on i) agents' ability to adapt to climatic changes through progressive accumulation of an assets a and ii) the adjustments to weather anomalies though a more intensive use of a. Note that this approach differs from the one adopted with Eq. (2), since the latter only provides a quantification of marginal effect of per capita income on the intensive margin adjustments, once the cross-sectional, long-term climatic effects on the intensive margin have been removed through a separate interaction effect.

We account for the influence of per capita income on both the intensive and extensive margin adjustments, and formulate an empirical specification that allows to adequately tests the model described in Eq. (4):

$$q_{i,t} \approx h(C_{i,t}, Y_{i,t}) + g(C_{i,t}, \omega_{i,t}; h(C_{i,t}, Y_{i,t})) \tag{10a}$$

$$\Rightarrow q_{i,t} = f(C_{i,t}) + f^Y(C_{i,t}) \cdot Y_{i,t} + z(\omega_{i,t}) + z^Y(\omega_{i,t}) \cdot Y_{i,t} + \mu_i + \sigma_t + \varepsilon_{i,t} \tag{10b}$$

3. Data and methods

3.1. Data

We adopt two mixed-frequency panel data-set covering, respectively, 28 European States over the period from 2006 to 2019 and 30 Indian States over the period from 2013 to 2019. The data-set include: (i) daily peak and total electricity load; (ii) daily population-weighted exposure to maximum temperatures, computed from hourly near surface temperature data at 0.25 degrees gridded resolution from ERA5 reanalysis (Hersbach et al., 2020); (iii) yearly state-level per capita GDP (Anon, 2021a,b). Data for 28 European States is taken from the European Network of Transmission System Operators (ENTSO-E), while data for 30 Indian States is collected from the Power System Operation Corporation (POSOCO). Actual total load is defined as the sum of power generated by plants on transmission networks, net of the balance (export–import) of exchanges on interconnections between neighboring bidding zones and the power absorbed by energy storage resources. The total load represents the power demand on the transmission and distribution networks, while any power demand served by distributed networks is not included in the statistics. Distributed generation reduces our measure of the total load at times of high generation from renewables. Despite such difference, throughout the paper we refer to load and electricity demand interchangeably.

3.2. Empirical models

Our empirical approach relies on two key elements. The first is the decomposition of the meteorological variable, daily maximum temperatures T, into two components: long-run climate normals and weather anomalies defined as deviations from those norms. We measure the climate normals ($\widetilde{C}_{i,d}$) as the 30-year moving average of the daily maximum temperature. For every day in the sample, $\widetilde{C}_{i,d}$ combines the information of the weather realizations of the previous 30 years in that same calendar day[1]. The adoption of a moving average assumes that individuals and firms respond to information on climatic variation they have observed and processed over the years[2]. The weather anomaly (ω_d) is computed as the deviation of daily maximum temperature from the 30-year average of maximum temperature. Weather shocks are computed as the difference between the observed weather exposure and the exposure expected by economic agents in each specific calendar day in the year:

$$\mathbb{E}(T_{i,d}|C_i) = \widetilde{C}_{i,d} = \frac{\sum_{n=j-31}^{j-1} T_{i,d}}{30} \tag{11}$$

$$\omega_{i,d} = T_{i,d} - \overline{C}_{i,d} \tag{12}$$

where: i indexes the State, d indexes the day, j indexes the year.

The second key element of our empirical approach is the estimation of the intensive and extensive margin components in the same equation by: i) exploiting variations that evolve slowly over time in each location to identify the average impact of long-run climatic changes, while controlling for time-invariant and time-specific observable variables though the fixed-effects; ii) retaining the high-frequency nature of the load-weather co-variation to capture fast responses of peak load to unexpected weather anomalies.

We characterize the response of per capita daily peak load to climate and weather anomalies by estimating a fixed-effect panel model in each of the two macro-regions, Europe and India. Variables are observed in State i and day d. For the clarity of notation, equations below omit regional and the time indices.

We test a first "naive" model specification including as main interest variable the observed daily maximum temperature exposure, binned into jth intervals (T_j). Temperature bins are a semi-parametric function that is widely adopted in order to capture non-linearities through the inclusion of piece-wise linear variables (as in Deschênes and Greenstone 2011, Auffhammer et al. 2017, De Cian and Sue Wing 2019Wenz et al. (2017)). The identification strategy relies on contemporaneous weather realizations, as previous panel studies (Wenz et al., 2017; Auffhammer et al., 2017). The effect on electricity demand in measured exclusively by the deviation of observed temperature from its local average value, and therefore β_j identifies shocks which are informative of the average short-run response across locations. Controls include per capita GDP and a matrix N including time and unit fixed-effects and a set of calendar dummies, see Eq. (17a).

The preferred specification uses two sets of covariates: i) the 30-year moving average of daily maximum temperature exposure binned into kth 3 °C intervals, denoted by the dummy indicators $D_{k,i,d}$; ii) the daily departure from these long-run averages, captured by the positive and negative temperature anomalies, $\omega^{+}_{i,d}$ and $\omega^{-}_{i,d}$, respectively[3]. We sort each daily observation into bins with a specific equidistant cut off of 3 °C and assign a value of one if daily average temperature falls in a given range[4]

$$D^{C}_{k} = \mathbb{1}[T_k \in (\underline{T}_k \widetilde{T}_k)] \tag{13}$$

$$k^{Europe} \in \{\langle 0, 0-3, \ldots, 27-30, \rangle 30\}, k^{India} \in \{\langle 12, 12-15, \ldots, 30-33, \rangle 33\} \tag{14}$$

$$D^{C}_{p(k)} = \mathbb{1}[T_{p(k)} \in (\underline{T}_{p(k)}, \widetilde{T}_{p(k)})], p(k) \in \{\langle 12, \rangle 24\} \quad \omega \in \{w^{-}_{i,d}, w^{+}_{i,d}\} \tag{15}$$

$$w^{+}_{i,d} = \begin{cases} T_{i,d} - \widetilde{C}_{i,d}, & T > \widetilde{C}_{i,d} \\ 0 & \text{otherwise} \end{cases} \quad w^{-}_{i,d} = \begin{cases} \widetilde{C}_{i,d} - T_{i,d}, & T < \widetilde{C}_{i,d} \\ 0 & \text{otherwise} \end{cases} \tag{16}$$

The effect of the weather anomalies from the climate is conditional on the temperature level. A given anomaly (e.g. +/- 1 °C) in a day with a hot climate norm (e.g. 28 °C) affects the response of the load demand differently than what the same anomaly does in a day with a cold climate norm (e.g. 12 °C). Therefore, weather anomalies are included in the equation through an interaction term with the climate variable, providing a flexible and asymmetric modulation of the linear piece-wise response of load (17b).[5].

Note that in Eq. (17b), income, measured by the logarithm of per capita GDP in the previous year, y, has no effect on the shape of the temperature response: it is simply a non-linear control that captures the adjustment of consumers' low-frequency conditional mean level of demand. In a set of alternative specifications we test if per capita income, affects the response of electricity demand to the climate and weather anomalies. In Eq. (17c) per capita income is assumed to interact only with the response of demand to climatically determined diurnal temperature maxima. This captures the situation in which the normal temperature regime induces agents to invest in stocks of energy-using space conditioning durable, but the extent to which agents respond through actual stock adjustments and average utilization levels is constrained by their income (as in Eq. (2)). The final specification includes a further interaction term between income and weather (Eq. (17d)), allowing to test the hypotheses that agents' ability to afford a more intensive use of existing energy-using stocks under a positive or negative temperature anomaly depends on their income (as in Eq. (3)).

$$q = \sum_{k} \gamma^{T}_{k} D^{T}_{k} + \beta^{Y} y + \mathbf{N}\boldsymbol{\beta}^{\mathbf{N}} + \varepsilon_1 \tag{17a}$$

[1] In an alternative specification we construct a monthly average of the 30-year moving average of daily maximum temperatures, in order to test if the inter-annual variation of our climate variable at different frequencies (daily or, alternatively, monthly) could affect the results. We find similar results for both specifications (see Supplementary Table 4 and 7), and therefore rely on the more general specification using a day-specific climate variable.

[2] We test alternative measure relying, respectively, on 10 and 20 years moving averages, finding negligible differences in the econometric model.

[3] An alternative specification uses month- ($D_{k,i,d}$) rather than calendar day-specific ($D_{k,i,m}$) variations in average climate. As we find no substantial differences between the two specifications, results are presented for the higher-frequency daily variable

[4] We conduct a set of robustness tests by adopting different cutoffs, ranging from 1.5 °C to 5 °C. We also test the reference temperature bin representing thermal comfort, by excluding from the regression equation alternatively the bins of the interval 15 °C-18 °C, 18 °C-21 °C and 21 °C-24 °C. We evaluate the performance of the different alternatives based on standard performance metrics (AIC, BIC) and find that the specification based on 3 °C is the one obtaining the best scores. The selected thermal comfort interval for Europe is 18 °C-21 °C while for India is 21 °C-24 °C.

[5] In order to reduce the number of variables included in the model, we test two alternative specifications: one in which weather anomalies are interacted with all climate bins k (see the Supplementary Informations) and one in which weather anomalies are interacted with two aggregated bins p capturing only the exposure to climatic norms below 15 °C and above 24 °C for Europe and below 15 °C and above 27 °C for India. As both specifications lead to very similar results (see the Supplementary Tables 3–6), we rely on the latter specification, providing a more aggregated but sufficiently flexible response function to weather anomalies. The results of all specifications are provided in the Supplementary Material (see the Supplementary Tables 1–7).

$$q = \sum_k \left(\gamma_k^C\right) D_k^C + \sum_{p(k)} D_{p(k)}^C \left[(\gamma_{p(k)}^w) w\right] + \beta^Y y + \beta^{YY} y^2 + \mathbf{N}\boldsymbol{\beta}^{\mathbf{N}} + \varepsilon_2 \quad (17b)$$

$$q = \sum_k \left(\gamma_k^C + \beta_k^C y\right) D_k^C + \sum_{p(k)} D_{p(k)}^C \left[(\gamma_{p(k)}^w) w\right] + \beta^Y y + \beta^{YY} y^2 + \mathbf{N}\boldsymbol{\beta}^{\mathbf{N}} + \varepsilon_3 \quad (17c)$$

$$q = \sum_k (\gamma_k^C + \beta_k^C y) D_k^C + \sum_{p(k)} D_{p(k)}^C \left[(\gamma_{p(k)}^w + \beta_{p(k)}^w y) w\right] + \beta^Y y + \beta^{YY} y^2 + \mathbf{N}\boldsymbol{\beta}^{\mathbf{N}} + \varepsilon_4 \quad (17d)$$

The coefficients γ_k^C capture the potentially nonlinear peak load response to climatically determined daily maximum temperature, while the coefficients γ_k^W capture the potentially asymmetric response of peak load to differences between each day's maximum temperature and the long-run normal maximum. The modulation of per capita income on the effects of climate and weather anomalies is estimated though the interaction coefficients β_k^C, β_k^W. The matrix N includes time and unit fixed effect, controlling, respectively, for unobserved unit-invariant and time-invariant confounders, as well as day-of-the-year, weekly, monthly and yearly fixed effects, to control for calendar and seasonal effects unrelated to temperature variations. Equations are estimated by OLS using White standard error robust to heteroscedasticity and, alternatively, Newey–West standard errors accounting for serial correlation. Our identification strategy allows to test if the response of q to a given observed maximum temperature $T = C_k + \omega_{p(k)}$, combining the extensive margin adjustment to C_k and the intensive margin adjustment to $\omega_{p(k)}$:

$$\gamma_{k'}^C + \beta_{k'}^C y \neq \gamma_k^C + \beta_k^C y + w(\gamma_{p(k)}^w + \beta_{p(k)}^w y) \quad (18)$$

In particular, if peak load response under a hotter climate C_k is higher than its response under the combination of the colder climate $C_{k'}$ and the positive anomaly $\omega_{k'}$, it suggests that adapting to the hotter climate increases the sensitivity of energy demand to temperature (for instance due to a variation in the stock of cooling appliances). The opposite would suggest that adapting to the hotter climate decreases the sensitivity of energy demand to the same observed maximum temperature T (for instance due to acclimatization or energy efficiency effects). A graphical representation of this comparison is provided in Fig. 1, for the case T = 30 °C, $C_{k'}$ = 27 °C, $\omega_{p(k')}$ +3 °C and C_k = 30 °C.

3.3. Climate change impact projections

For the projection component of our analysis, we use future estimates of global population and GDP downscaled to X-Y° grids from (Olen and Lehsten, 2022) and Murakami et al. (2021), respectively, developed in accordance with the shared socioeconomic pathway (SSP) scenarios. CDDs and daily maximum temperatures in current and mid-century climates are estimated using the outputs of 29 global climate models (GCMs) participating in the Coupled Model Intercomparison Project, Phase VI (CMIP6) (Eyring et al., 2016). Specifically, we use GCM-simulated daily temperature fields for moderate (SSP2-RCP45) and vigorous (SSP55-RCP85) warming scenarios that are bias corrected and downscaled to a 0.25° grid, from the NASA NEX-GDDP-CMIP6 dataset (Thrasher et al., 2012, 2022).

Baseline per capita peak electricity demand in 2050 is computed for each grid-cell by coupling the estimated income elasticities (ϕ and η) with the income per capita variations from 2010 to 2050 and the season-, month-, weekday- and country-specific fixed effects, in order to construct a baseline peak load profile specific for each day of the year. The second stage of our analysis combines the estimated parameters γ_k^C and β_k^C with climate change projections and per capita income projections, to estimate the impacts on the peak load of mid-century temperature increases along both the intensive and extensive margins.

We use representative 5-year periods from the current (2010–2014) and mid-century (2055–2059) epochs. Within each epoch we compute at the grid cell level (i), for each day (d), the contemporaneous maximum temperature interval, $\widetilde{C}_{i,d}^{Cur}$ and $\widetilde{C}_{i,d}^{Fut}$. Following Maraun (2016), climate change-driven temperature shifts were estimated by calculating the differences between simulated daily maximum temperatures over the historical and future epochs, and adding these "deltas" to the corresponding series of historical observations recorded in ERA5. The resulting synthetic series for the current and future epochs, $\widetilde{C_{i,d}}^{Cur}$, and $\widetilde{C_{i,d}}^{Fut}$, are then used to project the concomitant impact on daily peak load (ψ) in conjunction with Eq. (17d):

$$\psi = \frac{\exp\left[\sum_k \widehat{\gamma^C}_k^T \widetilde{C}^{Fut} + \sum_k \widehat{\beta^C}_k \left(\widetilde{C}_k^{Fut} \cdot \widetilde{y}^{Fut}\right) + \widehat{\beta}^Y \widetilde{y}^{Fut}\right]}{\exp\left[\sum_k \widehat{\gamma^C}_k^T \widetilde{C}_k^{Cur} + \sum_k \widehat{\beta^C}_k \left(\widetilde{C}_k^{Cur} \cdot \widetilde{y}^{Cur}\right) + \widehat{\beta}^Y \widetilde{y}^{Cur}\right]} \quad (19)$$

Eq. (19) is computed using each GCM's simulated output at the grid cell level (i) for the 5y epoch and constituent days (d), respectively. We leverage our observations of historical average per capita demand for i European countries and Indian states to aggregate the shocks using future gridded population, $\widetilde{n}^{Fut}$, as follows:

$$\Psi_i = \frac{\sum_{g(i)} \sum_d \psi_d \overline{q}_{i,d} \widetilde{n}_g^{Fut}}{\sum_{g(i)} \sum_d \overline{q}_{i,d} \widetilde{n}_g^{Fut}} \quad (20)$$

We decompose the variation in the additional electricity used for thermal comfort into the fractional effect of: i) the change in climate when actors are constrained by the current per capita income level ($\Psi^{intensive}$); the additional change resulting from the concomitant future climate and future per capita income ($\Psi^{extensive}$). We derive the amplification effect of future positive (π^+) and negative (π^-) weather anomalies on the peak load with respect to the historical climate based on Eqs. (21) and (22), respectively.

$$\pi^+ = \frac{\exp\left[\sum_k \widehat{\gamma^C}_k^T \widetilde{C}^{Fut} + \sum_k \widehat{\beta^C}_k \left(\widetilde{C}^{Fut} \cdot \widetilde{y}^{Fut}\right) + \sum_{p(k)} D_{p(k)}^{Fut} (\gamma_{p(k)}^w) w^+ + \widehat{\beta}^Y \widetilde{y}^{Fut}\right]}{\exp\left[\sum_k \widehat{\gamma^C}_k^T \widetilde{C}_k^{Cur} + \sum_k \widehat{\beta^C}_k \left(\widetilde{C}^{Cur} \cdot \widetilde{y}^{Cur}\right) + \widehat{\beta}^Y \widetilde{y}^{Cur}\right]} \quad (21)$$

$$\pi^- = \frac{\exp\left[\sum_k \widehat{\gamma^C}_k^T \widetilde{C}^{Fut} + \sum_k \widehat{\beta^C}_k \left(\widetilde{C}^{Fut} \cdot \widetilde{y}^{Fut}\right) + \sum_{p(k)} D_{p(k)}^{Fut} (\gamma_{p(k)}^w) w^- + \widehat{\beta}^Y \widetilde{y}^{Fut}\right]}{\exp\left[\sum_k \widehat{\gamma^C}_k^T \widetilde{C}^{Cur} + \sum_k \widehat{\beta^C}_k \left(\widetilde{C}^{Cur} \cdot \widetilde{y}^{Cur}\right) + \widehat{\beta}^Y \widetilde{y}^{Cur}\right]} \quad (22)$$

4. Results

Short- and long-run response functions

We find evidence of a statistically significant, U-shaped, relationship between peak electricity demand and the slowly varying climate exposure to maximum temperatures (see Supplementary Tables 1–7 in the Supplementary Material). The spline function resulting from the combination of the coefficients of the climate intervals (γ_k) increases more sharply in the temperature range for cooling services (around 24 °C and above) than for heating services (around 12 °C and below) both in Europe and India. The long-run response of the peak load to a shift in the climate from the reference interval to maximum temperatures above 30 °C is considerably higher in Europe (a 30% increase) than in India (an 11%–18% increase respectively in the intervals 30 °C - 33 °C and above 33 °C), when per capita income is fixed at the median level (black lines in the central panel of Fig. 2). In both Europe and India the long-run exposure to cold temperatures increases the peak by around 8%–10%. In India the left-arm of the response derives from the exposure to mild temperatures around 10 °C - 15 °C, suggesting that the underlying end-uses driving the shock are unrelated to residential

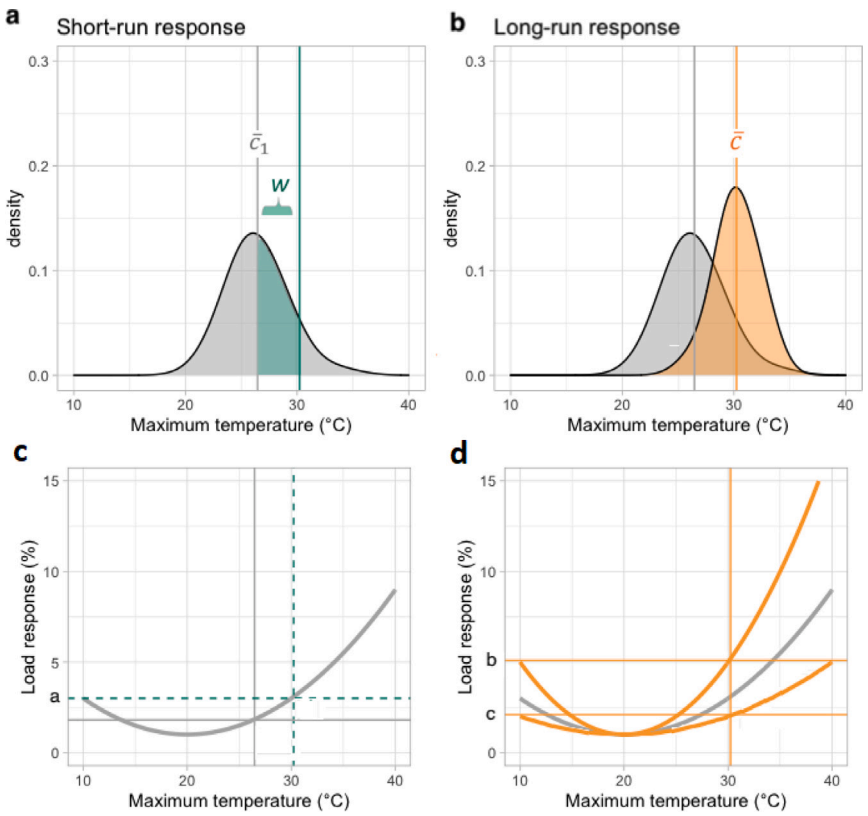

Fig. 1. Stylized short-run and long-run responses. Panel a shows a stylized distribution of daily maximum temperatures in a given calendar day, characterized by a mean value equal to C_1 and a weather shock equal to W_1, leading to an observed daily maximum temperature equal to T_2. Panel b shows how a shift in the stylized distribution of daily maximum temperatures translates into a variation in the local climate from C_1 to C. Panel c shows the load change due to the extensive margin response to C_1 and the intensive margin response to W_1. Panel d shows the load change due to the extensive margin response to C, alternatively higher (b) or lower (c) than the response in Panel C.

heating services and may derive from seasonal shifts in the power consumption of the agricultural and industrial activities that could not be captured though the fixed effects (such as the usage of ground water irrigation through electric pumps (Balasubramanian and Balachandra, 2021)).

In our preferred specification the long-run spline function is modulated by the short-run adjustment effect triggered by weather anomalies through the coefficients γ_k^W. The peak load response associated to any given maximum temperature realization T is not unique, but it depends on the underlying combination of the expected climate c and weather anomalies w. For any given $T > 24$ °C the *long-run* response lies above the set of *short-run* responses (colored scatters in Fig. 2): in other words, when the peak load is allowed to adjust in the long-run though the extensive margin, its sensitivity to hot temperatures increases. This result suggests that increasing air-cooling appliances' adoption is the driving underlying adaptation strategy to cope with an hotter climate. For any given $T < 15$ °C the *long-run* response lies within the set of *short-run* responses, suggesting that the sensitivity of peak electricity demand to heating needs may be reduced over time. Variations over time in the energy efficiency of appliances and better home insulation may be factors that contribute to such effect[6]. Per capita income modulates both the long-run response of the peak load across the full set of bins k, and the short-run response to positive weather anomalies occurring above 24 °C for Europe and 27 °C for India, altering significantly both the *short-run* and *long-run* responses (Fig. 2). The shocks associated with maximum temperatures above 30 °C in Europe and above 33 °C in India more than double when per capita income shifts to the 75th quantile (12,000 USD/year for Europe and 1,100 USD/year for India) from the 25th quantile (37,000 USD/year for Europe and 2,700 USD/year for India). We find that the high-income response of India approaches the low-income response of Europe, despite the large differences in nominal income per capita between the two regions.

Regional impact of climate shifts and weather anomalies

The shift from the historical daily maximum temperature exposure to the future climatic exposure around 2050 triggers a change in the *long-run* - optimal - response of the peak load. When we aggregate the shocks from the gridcell-level to the macro-regional level, we find a *long-run* increase of the peak load of up to 12% in Europe and 15% in India (black line in Fig. 3, Panel a) under the RCP 5-8.5 (differences across SSPs and RCPs are presented in the Supplementary Material). The *long-run* shocks, that represent the adjustments driven by slowly changing climatic exposure and include the amplification effect of income growth (see Eq. (17d)), are roughly two times larger than the shocks computed based on the naive weather response function (Eq. (17a), dotted line in Fig. 3, Panel a). Taking into account the latent, extensive margin, adjustments changes considerably the projected impact of climate change on the peak load. On top of the shift in the climatic norm, we quantify the additional influence of future positive and negative anomalies from that norm. In other words, we consider how the peak load responds not only the shift in the mean of the distribution (based on the extensive margin response) but also to the dispersion around that mean (based on the intensive margin

[6] The set of *short-run* responses is computed for each maximum temperature bins T_q (with a 1 °C interval width) by taking into account any combinations of C and ω observed in the sample that would result in a value within T_q. In other words, the distribution of the observed C and ω in the sample is used to construct the distribution of possible *short-run* responses for any given T_q.

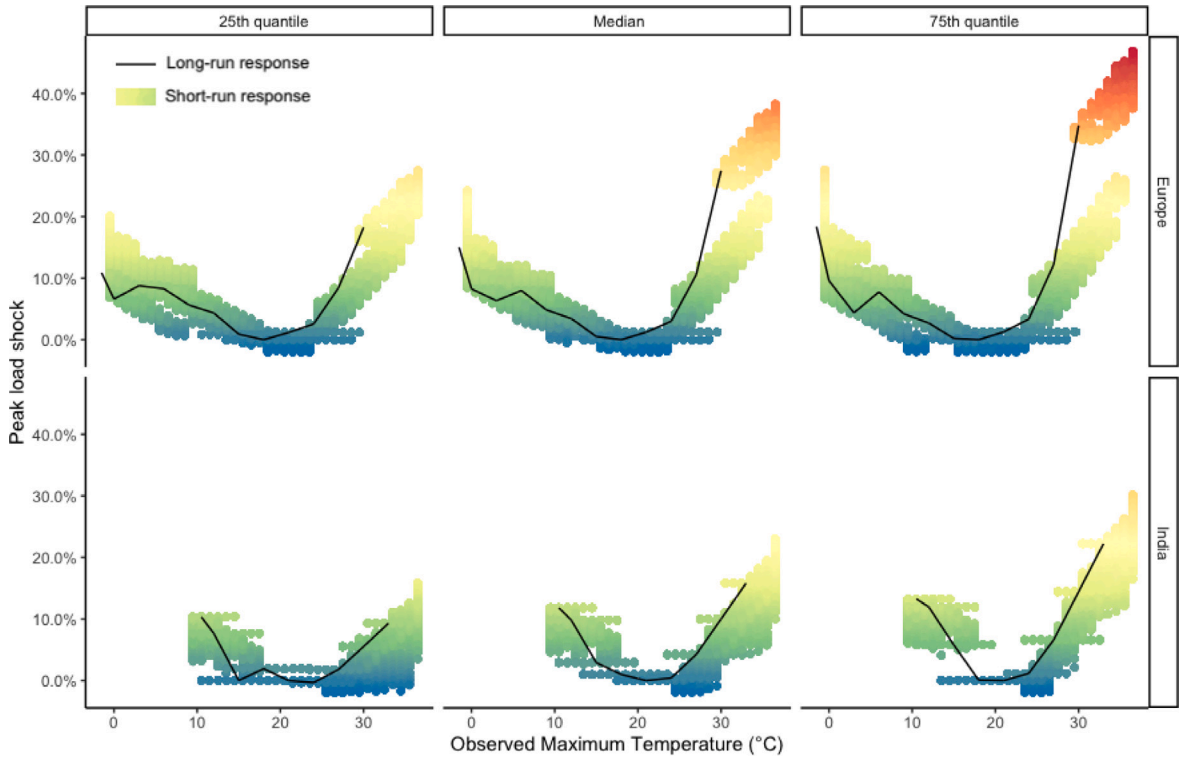

Fig. 2. Long- and short-run adaptation responses to maximum temperature exposure by per capita income quantile. The long-run adaptation response (black line) is presented next to the short-run response for each 1 °C bin of maximum temperature exposure (colored scatters). The range of short-run responses is computed, for each 1 °C bin of maximum temperature exposure, from the distribution of the weather anomalies and climate norms in the two regions' samples. Coefficients are estimated though Eq. (8)-d.

response). We estimate the additional impact of the occurrence of weather anomalies by computing the standard deviation of all future maximum temperatures anomalies for any given calendar day and location (projected by 25 GCMs in each calendar day for the period 2040-2060[7]). Light red (blue) shades represent the resulting shock obtained by adding (subtracting) one standard deviation of the anomaly to the climatic exposure, in each calendar day. We find that the pressures on the electric grid can be greatly amplified by the combination of shifts in the mean climate and weather anomalies[8]: positive weather anomalies can result in a peak load shock of 20% in both Europe and India under the RCP 8.5.

Patterns in the North-South gradient

The impact of climate change on peak demand across the two regions is affected by the seasonal and geographical heterogeneity across states. In Europe, a predominantly temperate region, we identify a strong North-South gradient: Northern European countries experience reductions in the peak load of up to −20% due to milder winters, while Southern countries experience an exacerbation of summer peaks of up to 20% (33%), excluding (including) the additional effect of positive weather anomalies (Fig. 4, Panel a). A similar gradient is present in India, a predominantly tropical region, where states located in the Northern areas (Jammu and Kashmir, Himachal Pradesh, Sikkim) experience reductions in the peak load in the winter but, at the same time, non-negligible increases in the peak load in the summer. A second group of States located in the Central ans Southern regions experience a similar evolution of shocks, mostly happening after the end of the dry season (December-March) (Fig. 4, Panel a). Delhi and Goa are the states with the highest relative increase in daily peak load, reaching values around 30% (33%), excluding (including) the additional effect of positive weather anomalies. The difference in the extent of the gradient in Europe and India derives from the inherently different tropical and temperate climates in the two regions, which are reflected also in the reduced-form responses of peak load. We find that in areas close to the equator the response to heat is characterized by an almost monotonic function, given that the range of the daily average maximum temperatures distribution, between 24 °C and 40 °C, corresponds only to the rightward arm of the response function identified for India. On the other hand, in temperate regions the response exhibits the typical U-shaped form as the daily average maximum temperatures distribution ranges from roughly 0 °C to over 30 °C. This difference results in a weakening of the North-South gradient when extending towards the tropics, as the heterogeneity in the response across regions saturates. In other words, we show that the gradient effect is not monotonically increasing all the way to the equator.

Increase in the annual peak capacity

Although we project the amplification in the peak load over the full extent of a year, capacity planning relies on the long-run projections of the maximum peak load in a year (henceforth "annual peak"). Here we provide a quantification of the annual peak around 2050 due to both socio-economic growth and climate change. The variations in per capita income and population from the current period to 2050 trigger

[7] For any given calendar days in any location, the distribution of weather anomalies from the climate norm comprises 420 values

[8] The additional intensive margin component is computed assuming that in a given calendar day all locations experience a temperature which is equal to the climate norm plus/minus one standard deviation of the maximum temperature projected in the years 2050 to 2059, meaning that we show a scenario in which in the same day everywhere in Europe and India weather is warmer than the 30 years' average. The aggregation from grid-cell to country shocks is based on population share, as we assume that power demand within a country is exactly proportional to its population. The aggregation from the National to the regional level is based on the share of National peak demand over the regional total in 2019.

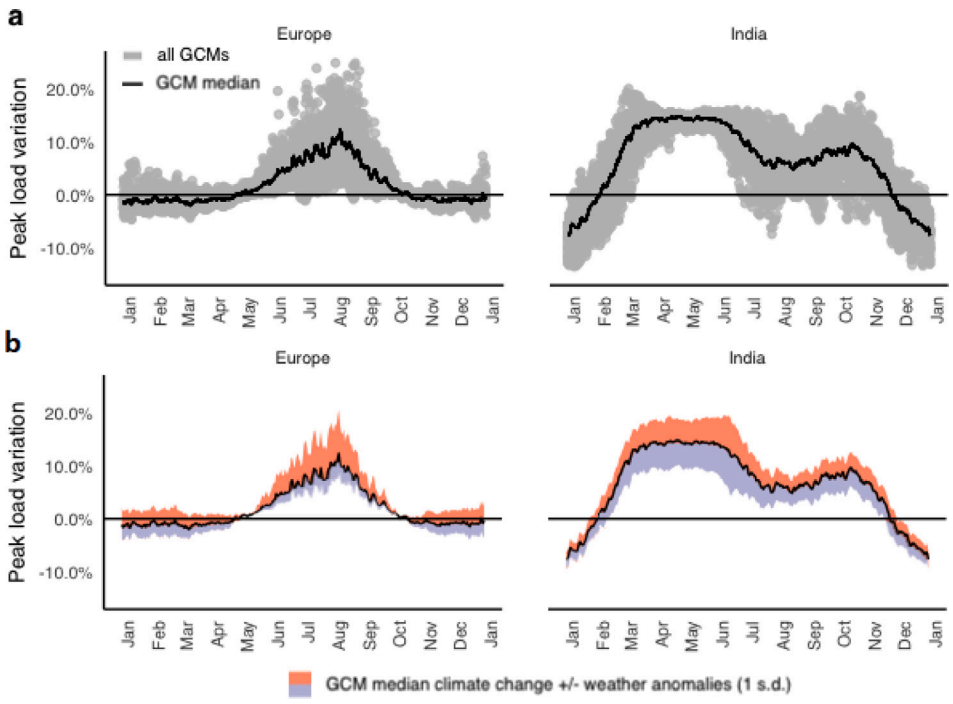

Fig. 3. Macro-regional peak load response due to climate change around 2050 under RCP 5-8.5. Panel a: Percentage increase in the peak load due to mean climate shifts in each day of the year circa 2050 for each of 25 GCMs (scatters) and mean across GMCs (black lines). The mean shock based on the model with climate coefficients (solid black line) is compared to the mean shock based on the weather model (dotted black line). Panel b: Percentage increase in the peak load due to the combined effect of mean climate shifts (solid black line) and weather anomalies (colored shades). Light red (blue) shades represent the weather anomaly component obtained by adding (subtracting) one standard deviation of the daily maximum temperature from the climatic exposure, computed for each calendar day, as the mean across 25 GCMs.

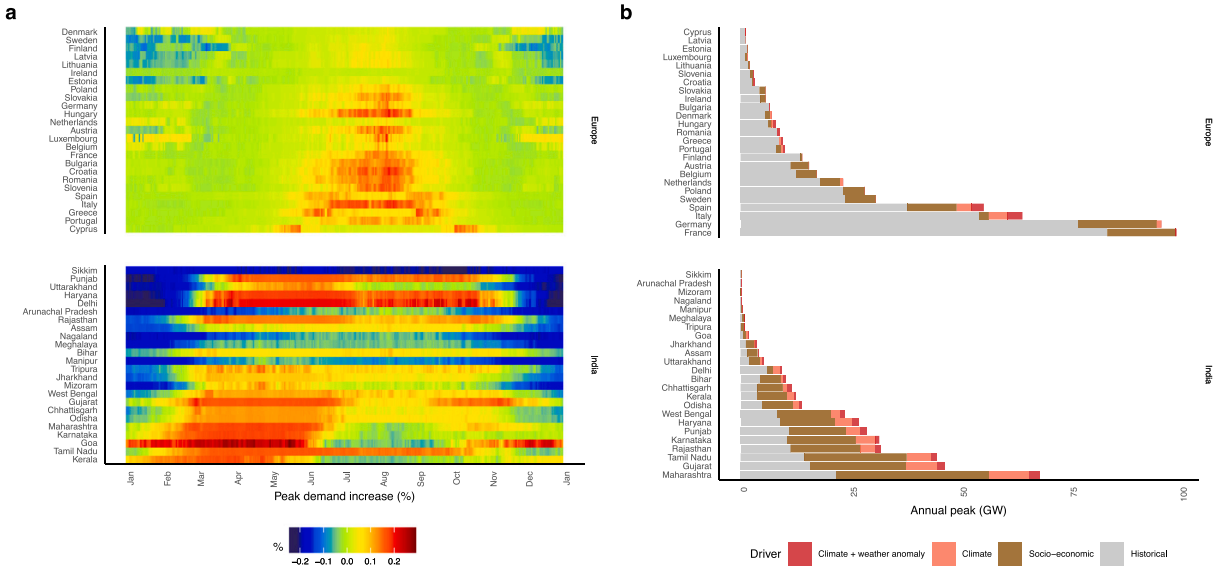

Fig. 4. Panel a: Peak load shock induced by climate change shifts, by day of the year circa 2050 under RCP 5-8.5. The values correspond to the mean across 25 GCMs. Panel b: Annual peak load in 2050, decomposed between four additive components: i) historical annual peak load (highest level observed in the time series), ii) additional increase due to the income per capita growth, under the RCP 5-8.5., iii) additional increase due to climate change and iv) due to a positive weather anomaly, under the RCP 5-8.5.

an increase in the future annual peak that is independent from the influence of climate change ("socio-economic driver"). The baseline annual peak in 2050 increases considerably with respect to the historical level in the Indian states experiencing large growth in both per capita income and population. In India, we project that an additional 185 GW of annual peak demand will be required (a 140% increase from the historical annual peak), while 80 GW will be required in Europe (a 19% increase from the historical annual peak), under the RCP 5-8.5. The impact of climate change on the maximum annual peak load derives from the combination of two different drivers: i) the climatic shifts in the moving average of daily maximum temperatures; ii) the additional peak demand due to future positive weather anomalies departing from

the average climatic exposure(Fig. 4, Panel b)[9]. Together, the shifts in the climate norm and weather anomalies account for an increase in the annual peak of roughly 20 GW in Europe and 60 GW in India, mostly due to the additional requirements in a handful of Southern European states (Italy 8 GW and Spain 6 GW) and Indian states (Maharashtra 12 GW, Gujarat 9 GW, Tamil Nadu 6 GW). The additional annual peak is indicative of demand-side shocks prior to any market adjustment. The analysis of the implications of such ex-ante demand shifts on the supply-side (i.e. on electricity generation, dispatch and transmission) requires the adoption of power market and capacity expansion models that fall beyond the scope of this study.

5. Discussion

A small number of studies indicate how the peak load of developed countries responds to intensive margin adjustments. In the United States, the peak load is expected to vary due to increases in daily average temperatures by moderate and heterogeneous changes, with an average increase of 3.5% (9.6%) under the RCP 4.5 (RCP 8.5) by 2100 (Auffhammer et al., 2017). In Europe, substantial heterogeneity across regions has been identified, with shocks as low as −4% (−6%) in Northern countries and +4% (+8%) in Southern countries around 2050 (2100) under the RCP 8.5 (Wenz et al., 2017). The range of shocks provided for the European countries in Wenz et al. (2017) is in line with our projections based on the model specification excluding any long-run adjustment or per capita income modulation effect (a 5% to 8% increase in the peak load in Western and Southern European states in 2050 under RCP 8.5, see Supplementary Figure 3). Our specification based on the extensive margin provides substantially higher relative changes in peak demand already around 2050, due to the long-run adjustments to climate and the additional short-run adjustments to weather anomalies. Our results shed light on the fact that changes in electricity demand due to climate change adaptation are going to be driven by movements along the extensive margin, a component disregarded by the previous studies based on peak load data (Wenz et al., 2017; Auffhammer et al., 2017) and that has been addressed more often by studies exploiting billing data and households' information (Auffhammer, 2022b; Davis and Gertler, 2015)). Our projections are inclusive of the amplification effect of per capita income on the sensitivity of peak load, an effect that has so far been identified only by studies using more aggregated energy statistics (Rode et al., 2021; Colelli and Mistry, 2022) or micro-level surveys (Pavanello et al., 2021).

Colelli et al. (2023) is the only study directly comparable, as it provides an estimation of the effect of adaptation on the peak load through future variations in residential AC ownership (i.e. directly measuring extensive margin adjustments), using a dataset with similar geographic and temporal scope. With respect to Colelli et al. (2023), the relative increases of the peak load we project have a similar magnitude in both Europe and India, pointing to the adequacy of our income-modulation and long-run climatic effects as proxies for extensive margin adjustments when data on AC is not available (see Supplementary Figure 4). Nevertheless, some differences between our projections and Colelli et al. (2023) arise, as the former appear to be higher than the latter in colder states (such as Germany and France) while higher in hotter states (such as Italy and Spain). Such differences might arise because future income per capita amplifications increase the sensitivity of the peak load to both hot temperatures and cold temperatures, while in Colelli et al. (2023) AC ownership amplifications only affect cooling demand. Furthermore, peak load shocks in Colelli et al. (2023) are based on variations in residential AC ownership rates, while our shocks are based on income and climatic variables that capture economy-wide extensive margin adjustments.

Through the decomposition between climate and weather anomalies, we obtain a long-run response to high temperatures that is the outer envelope of short-run possibilities, a result that is in line with alternative methodological frameworks measuring adaptation with panel data (Mérel and Gammans, 2021). Note that while Mérel and Gammans (2021) develop a framework that by design imposes that the long-run curve lies above the short-run curve, we do not impose any such restriction. As a result, we find that: i) the long-run peak load response for heating services lies within the short-run response, pointing to an attenuating effect over the long-run; ii) the long-run peak load response for cooling services is always above the short-run response, and we explain this adaptation dynamic by the fixity of cooling appliances' purchases in the short-run. Although we cannot identify the specific end-uses underlying the short- and long- term responses, the drivers of such adjustments can in part be attributed to shifts in the residential and commercial sectors' adaptation actions, ranging from adoption of new appliances to efficiency improvements and changes in buildings' insulation. Lack of information on the sector-level high-frequency electricity demand prevents us from identifying adjustments that separate buildings' cooling and heating demands from weather-sensitive end uses in other sectors, in particular from the consumption of industrial and agricultural activities. Industries use heating, ventilation, and air-conditioning (HVAC) systems both for ensuring thermal comfort of workers and for process-related purposes (the latter ensuring that the operation of manufacturing systems and production processes is not undermined by temperature variations (Murphy et al., 2007)), while electricity demand from agriculture comes from irrigation activities (Balasubramanian and Balachandra, 2021). Electricity consumption for these activities may depart from the seasonal average consumption, that we control for through the use of flexible fixed-effects, due to the intensification of HVAC or irrigation needs and due to possible drops in the energy efficiency of the industrial and irrigation systems during extreme heat events or droughts (Soto-García et al., 2013). Furthermore, shifts from short- to long-run electricity demand due to adaptation may occur also in industrial and agriculture activities, through the acquisition of new machinery or shifts in practices and type of crops (Wing et al., 2021). Therefore, it is likely that our findings identify the combined shifts from the short- to the long-run sensitivity of peak load of different responses across sectors, which so far have been separated only though time-aggregated annual energy statistics (De Cian and Sue Wing, 2019).

The difference between the long-run and short-run response is robust across two very different regions. Despite macro-level studies suggest that historical temperature responsiveness of electricity demand in the tropics is small (De Cian and Sue Wing, 2019), studies based on micro-data show that growth in air conditioner penetration in tropical countries will increase cooling electricity requirements (Davis and Gertler, 2015). By exploiting state-level electricity demand statistics we find evidence backing the latter hypothesis.

Even with a limited scope to two world regions, we identify that the structure of the economy and differences in future income growth matter in shaping the peak load amplification due to climate change. The extensive margin shock is going to be very relevant in places that already have high levels of income through the temperature channel, as well as in hot places that are poor though the income growth channel. Whether this evidence is indicative of a pattern that can be extended to other world regions is nonetheless a speculative assumption. More data are needed to investigate the extent to which these patterns are robust in areas such as South America, East Asia and Africa. High frequency (daily, hourly) electric load data for sub-national administrative units are now routinely archived in several countries in and outside of OECD, expanding the scope for future research on world regions for which empirical evidence is lacking. The adoption of our model to

[9] Results of the state-level peak capacity projections around 2050 by SSP and RCP are provided as a Supplementary Data file.

other contexts can be limited by one key data requirement: since our framework relies on the slowly-evolving climatic exacerbation in each location, an insufficiently long time span of the panel data can hider the identification of climate variations over time.

6. Conclusions

This paper proposes a new methodology for the assessment of climate change adaptation that has two main advantages: i) through the variation that evolves slowly over time in each location we identify the average impact of long-run climatic changes, our analogue for the extensive margin adjustment, without an explicit measurement of the ownership shares of air conditioners and controlling for time-invariant and time-specific unobservables; ii) we retain the high frequency nature of the load-weather co-variation, enabling to capture the fast responses of peak load to unexpected weather anomalies, our analogue for the intensive margin adjustments. Thanks to this decomposition we show that both an increase in the maximum temperatures' climate norms and the inherent unexpected variation around that norms can contribute to increase the pressure on the peak load in Europe and India, with respect to historical climate conditions.

We leave for future work the adoption of a weather variable accounting for humidity (i.e. daily maximum wet-bulb temperature), and the inclusion of a wider set of controls for seasonal economic activities (quarterly or monthly macroeconomic data at the State level in India is unavailable from public repositories to the best of our knowledge). A further improvement would be accounting for differences in the long-run response function across sectors, as the available evidence based on more aggregated energy demand statistics shows considerable heterogeneity between the residential, commercial, and industrial sectors (De Cian and Sue Wing, 2019; Colelli and Mistry, 2022),

Our key impact metric quantifies the relative effects of future socio-economic and climatic shifts on the peak load by assuming that today's structure of the power market is maintained towards 2050. Our projections depend on the assumption that the historical diffusion of appliances, as well as their average energy efficiency, can be an appropriate measure of the evolution of the extensive margin in the future. The adoption of energy efficient appliances at a rate higher than the historical one, as well as breakthrough technological changes, can lower the peak demand required to satisfy heating and cooling needs (e.g. though the large scale adoption of green roofs or demand side management mechanisms targeting consumption during heat waves). Furthermore, we do not account for the implications on the supply-side, most importantly on the power generation options that could meet the projected increase in the peak load (ranging from conventional thermal generation, storage and variable renewable energy), nor the potential limitations deriving from grid constraints. The implications for power supply, costs, reliability, and carbon emissions can be evaluated only by coupling the high-frequency shocks estimated in this work with capacity expansion and dispatch models.

CRediT authorship contribution statement

Francesco Pietro Colelli: Methodology, Investigation, Data curation, Writing – original draft. **Ian Sue Wing:** Methodology, Writing – review & editing. **Enrica De Cian:** Conceptualization, Methodology, Writing – review & editing.

Acknowledgments

F.P.C and E.D.C. were supported by the European Research Council (ERC) under the European Union's Horizon 2020 research and innovation programme under grant agreement No. 756194 (ENERGYA) and by the H2020-MSCA-RISE project GEMCLIME-2020, grant agreement No. 681228. ISW was supported by U.S. Department of Energy, Office of Science, Biological and Environmental Research Program, Earth and Environmental Systems Modeling MultiSector Dynamics Cooperative Agreement DE-SC0022141. The authors would like to thank David Anthoff, Antonio Bento, Lucas Davis and Maximilian Auffhammer for their constructive comments and feedback.

Appendix A. Supplementary data

Supplementary material related to this article can be found online at https://doi.org/10.1016/j.eneco.2023.106923.

References

Anon, 2021a. Eurostat database. https://ec.europa.eu/eurostat/data/database.

Anon, 2021b. National poertal of India state statistics. https://ec.europa.eu/eurostat/data/database.

Aroonruengsawat, Anin, Auffhammer, Maximilian, 2011. Impacts of Climate Change on Residential Electricity Consumption. University of Chicago Press.

Auffhammer, Maximilian, 2022a. Climate adaptive response estimation: Short and long run impacts of climate change on residential electricity and natural gas consumption. J. Environ. Econ. Manag. 102669.

Auffhammer, Maximilian, 2022b. Climate adaptive response estimation: Short and long run impacts of climate change on residential electricity and natural gas consumption. J. Environ. Econ. Manag. 114, 102669. http://dx.doi.org/10.1016/j.jeem.2022.102669, URL https://www.sciencedirect.com/science/article/pii/S0095069622000432.

Auffhammer, Maximilian, Baylis, Patrick, Hausman, Catherine H., 2017. Climate change is projected to have severe impacts on the frequency and intensity of peak electricity demand across the United States. Proc. Natl. Acad. Sci. 114 (8), 1886–1891.

Auffhammer, Maximilian, Mansur, Erin T., 2014. Measuring climatic impacts on energy consumption: A review of the empirical literature. Energy Econ. 46, 522–530.

Balasubramanian, S., Balachandra, Patil, 2021. Characterising electricity demand through load curve clustering: A case of karnataka electricity system in India. Comput. Chem. Eng. 150, 107316.

Barnett, Jon, O'Neill, Saffron, 2010. Maladaptation. Pergamon.

Bento, Antonio, et al., 2020. A Unifying Approach to Measuring Climate Change Impacts and Adaptation. Tech. Rep., National Bureau of Economic Research.

Bento, Antonio, et al., 2021. Time is of the Essence: Climate Adaptation Induced by Existing Institutions. Tech. Rep., National Bureau of Economic Research.

Boßmann, T., Staffell, Iain, 2015. The shape of future electricity demand: Exploring load curves in 2050s Germany and Britain. Energy 90, 1317–1333.

Burke, Marshall, Emerick, Kyle, 2016. Adaptation to climate change: Evidence from US agriculture. Am. Econ. J.: Econ. Policy 8 (3), 106–140.

Burke, Marshall, Hsiang, Solomon M., Miguel, Edward, 2015. Global non-linear effect of temperature on economic production. Nature 527 (7577), 235–239.

Butler, Ethan E., Huybers, Peter, 2013. Adaptation of US maize to temperature variations. Nature Clim. Change 3 (1), 68–72.

Carleton, Tamma A., et al., 2020. Valuing the Global Mortality Consequences of Climate Change Accounting for Adaptation Costs and Benefits. Tech. Rep., National Bureau of Economic Research.

Colelli, Francesco, Mistry, Malcolm, 2022. Income-dependent expansion of electricity demand for climate change adaptation in Brazil. Energy Clim. Change 100071.

Colelli, Francesco Pietro, Wing, Ian Sue, Cian, Enrica De, 2023. Air-conditioning adoption and electricity demand highlight climate change mitigation–adaptation tradeoffs. Sci. Rep. 13 (1), 4413.

Davis, Lucas W., Gertler, Paul J., 2015. Contribution of air conditioning adoption to future energy use under global warming. Proc. Natl. Acad. Sci. 112 (19), 5962–5967.

Davis, Lucas, Gertler, Paul, Jarvis, Stephen, Wolfram, Catherine, 2021. Air conditioning and global inequality. Global Environ. Change (ISSN: 09593780) 69 (July 2020), 102299. http://dx.doi.org/10.1016/j.gloenvcha.2021.102299.

De Cian, Enrica, Sue Wing, Ian, 2019. Global energy consumption in a warming climate. Environ. Resource Econ. 72 (2), 365–410.

Dell, Melissa, Jones, Benjamin F., Olken, Benjamin A., 2014. What do we learn from the weather? The new climate-economy literature. J. Econ. Lit. 52 (3), 740–798.

Deschênes, Olivier, Greenstone, Michael, 2011. Climate change, mortality, and adaptation: Evidence from annual fluctuations in weather in the US. Am. Econ. J.: Appl. Econ. 3 (4), 152–185.

Eyring, Veronika, et al., 2016. Overview of the coupled model intercomparison project phase 6 (CMIP6) experimental design and organization. Geosci. Model Dev. 9 (5), 1937–1958.

Fonseca, Francisco Ralston, et al., 2019. Seasonal effects of climate change on intra-day electricity demand patterns. Clim. Change 154 (3), 435–451.

Hersbach, Hans, et al., 2020. The ERA5 global reanalysis. Q. J. R. Meteorol. Soc. 146 (730), 1999–2049.

Hsiang, Solomon M., et al., 2016. Climate Econometrics.

International Energy Agency, 2018. The Future of Cooling. IEA, Paris.

Kolstad, Charles D., Moore, Frances C., 2020. Estimating the economic impacts of climate change using weather observations. Rev. Environ. Econ. Policy 14 (1), 1–24.

Lindberg, K.B., et al., 2019. Long-term electricity load forecasting: Current and future trends. Util. Policy 58, 102–119.
Maraun, Douglas, 2016. Bias correcting climate change simulations-a critical review. Curr. Clim. Change Rep. 2 (4), 211–220.
Mendelsohn, Robert, Nordhaus, William D., Shaw, Daigee, 1994. The impact of global warming on agriculture: A Ricardian analysis. Am. Econ. Rev. 753–771.
Mérel, Pierre, Gammans, Matthew, 2021. Climate econometrics: Can the panel approach account for long-run adaptation? Am. J. Agric. Econ. 103 (4), 1207–1238.
Moore, Frances C., Lobell, David B., 2014. Adaptation potential of European agriculture in response to climate change. Nature Clim. Change 4 (7), 610–614.
Moral-Carcedo, Julián, Pérez-García, Julián, 2017. Integrating long-term economic scenarios into peak load forecasting: An application to Spain. Energy 140, 682–695.
Murakami, Daisuke, Yoshida, Takahiro, Yamagata, Yoshiki, 2021. Gridded GDP projections compatible with the five SSPs (shared socioeconomic pathways). Front. Built Environ. 7, 760306.
Murphy, Rose, Rivers, Nic, Jaccard, Mark, 2007. Hybrid modeling of industrial energy consumption and greenhouse gas emissions with an application to Canada. Energy Econ. 29 (4), 826–846.
Olen, Niklas Boke, Lehsten, Veiko, 2022. High-resolution global population projections dataset developed with CMIP6 RCP and SSP scenarios for year 2010–2100. Data Brief 40, 1–7.
Pavanello, Filippo, et al., 2021. Air-conditioning and the adaptation cooling deficit in emerging economies. Nat. Commun. 12 (1), 1–11.
Rode, Ashwin, et al., 2021. Estimating a social cost of carbon for global energy consumption. Nature 598, 308–314.
Romitti, Y., Sue Wing, I., 2020. Mid-century temperature shifts' heterogeneous impacts on the demand for electricity: Evidence from world cities. In: AGU Fall Meeting Abstracts, Vol. 2020. pp. GC073–0013.
Schlenker, Wolfram, Hanemann, W. Michael, Fisher, Anthony C., 2005. Will US agriculture really benefit from global warming? Accounting for irrigation in the hedonic approach. Amer. Econ. Rev. 95 (1), 395–406.
Schlenker, Wolfram, Roberts, Michael J., 2006. Nonlinear effects of weather on corn yields. Rev. Agric. Econ. 28 (3), 391–398.
Schlenker, Wolfram, Roberts, Michael J., 2009. Nonlinear temperature effects indicate severe damages to US crop yields under climate change. Proc. Natl. Acad. Sci. 106 (37), 15594–15598.
Seneviratne, Sonia I., et al., 2021. 11 Chapter 11: Weather and climate extreme events in a changing climate.
Soto-García, M., et al., 2013. Energy consumption for crop irrigation in a semiarid climate (south-eastern Spain). Energy 55, 1084–1093.
Stone, Jr., Brian, et al., 2023. How blackouts during heat waves amplify mortality and morbidity risk. Environ. Sci. Technol..
Thrasher, Bridget, Maurer, Edwin P., et al., 2012. Bias correcting climate model simulated daily temperature extremes with quantile mapping. Hydrol. Earth Syst. Sci. 16 (9), 3309–3314.
Thrasher, Bridget, Wang, W., Melton, A., Lee, F., Nemani, R., 2022. NASA global daily downscaled projections, CMIP6. Nat. Sci. Data 9 (1), 262.
Wenz, Leonie, Levermann, Anders, Auffhammer, Maximilian, 2017. North–south polarization of European electricity consumption under future warming. Proc. Natl. Acad. Sci. 114 (38), E7910–E7918.
Wing, Ian Sue, De Cian, Enrica, Mistry, Malcolm N., 2021. Global vulnerability of crop yields to climate change. J. Environ. Econ. Manag. 109, 102462.
Yalew, Seleshi G., et al., 2020. Impacts of climate change on energy systems in global and regional scenarios. Nat. Energy 5 (10), 794–802.